Selective Particle Distribution and Mechanical Properties of Nano-$CaCO_3$/Ethylene-Propylene-Diene Terpolymer/Polypropylene Composites with High Content of Nano-$CaCO_3$

Xu Wang,[1] Ke-Jie Xu,[1] Xiang-Bin Xu,[1] Soo-Jin Park,[2] Seok Kim[2]

[1]*College of Chemical Engineering and Materials Science, Zhejiang University of Technology, Hangzhou, Zhejiang 310014, People's Republic of China*
[2]*Advanced Materials Division, Korea Research Institute of Chemical Technology, Yusong, Daejeon 305-600, South Korea*

Received 8 July 2008; accepted 17 January 2009
DOI 10.1002/app.30078
Published online 28 April 2009 in Wiley InterScience (www.interscience.wiley.com).

ABSTRACT: Ternary composite of nano-$CaCO_3$/ethylene-propylene-diene terpolymer (EPDM)/polypropylene (PP) with high content of nano-$CaCO_3$ was prepared by two step compounding route, in which EPDM and nano-$CaCO_3$ were mixed first, and then melt compounding with PP matrix. The influence of mixing time during the second compounding on distribution of nano-$CaCO_3$ particles and the impact strength of the ternary composite have been investigated. It was found that the Izod impact strength of composite decreased with increasing mixing time. The observation of transmission electron microscopy obviously showed that nano-$CaCO_3$ particles transported from EPDM to PP matrix firstly and then from PP to the vicinity of EPDM dispersed phase with the increase of mixing time. This phenomenon can be well explained by the minimization of the dissipative energy and the Young's equation. The scanning electron microscope images show that lots of nano fibrils exist at the interface between nano-$CaCO_3$ agglomerates and matrix, which can dissipate lots of energy. The toughening mechanism has been interpreted in terms of three-stage-mechanism: stress concentration, void and shear band formation, and induced shear yielding. © 2009 Wiley Periodicals, Inc. J Appl Polym Sci 113: 2485–2491, 2009

Key words: poly(propylene); nanocomposites; selective distribution; interfacial tension; toughness

INTRODUCTION

Polypropylene (PP) is widely used in packing, textiles, common household, and automobile because of its good processability, relatively comprehensive performance, cheapness, and so forth. However, its poor toughness, especially at low temperature and in the presence of notches, restricts its applications in many fields. Thus, it is meaningful to enhance the toughness of PP for both academia and business circles.[1]

Among the different methods used to enhance the toughness of polymer materials, the addition of elastomer is the most successful way although accompanying with the decrease of overall stiffness. Conversely, rigid fillers are usually used to improve the modulus of the matrix whereas with the decrease of impact strength. To achieve an optimum balance of impact strength and stiffness, researchers now pay attention to the inorganic filler/elastomer/PP ternary composites.[2–14] Ma et al.[3] studied PP/ethylene-octene copolymer (POE)/nano-$CaCO_3$ composites and found that the core-shell structure was formed in the matrix, which can increase the impact strength of PP. The increase of the effective volume fraction for the dispersed phase in the ternary composites was found to be the reason for the toughness increment. In the study by Premphet et al.,[7] separate dispersed phases and core-shell structures were found in PP/ethylene-octene copolymer (EOR)/$CaCO_3$ and PP/ethylene-vinyl acetate (EVA)/$CaCO_3$, respectively, which was attributed to the higher affinity between EVA and calcium carbonate. Yang et al.[10] studied PP/ethylene-propylene-diene terpolymer (EPDM)/nano-SiO_2 composites. They found that the filler-network structure could form in PP/EPDM/nano-SiO_2 composites by taking two-step processing method, which is a key role for increasing toughness and moduls of PP simultaneously.

It is well known that some of the nano-inorganic fillers such as nano-$CaCO_3$ have relatively low price compared with the polymer matrix. Thus, the composites with high content of nano-inorganic filler

Correspondence to: Xu Wang (wangxu@zjut.edu.cn).
Contract grant sponsor: Nature Science Foundation of China; contract grant number: 50573067.
Contract grant sponsor: International Scholar Exchange Fellowship (ISEF) of the Korea Foundation for Advanced Studies (KFAS).

usually have economical cost than that with low content of filler. In view of these previous works on nano-inorganic filler/elastomer/PP composites, the content of nano-inorganic filler in almost all systems is less than 15% in weight.[3,10,15] It is really of great importance to explore the relationship between the microstructure and properties of these ternary composite with high content of nano-inorganic filler. In our previous works,[4] the compounding route of nano-$CaCO_3$/EPDM/PP composites and the influences on their properties were studied. It was found the composite prepared by two-step compounding route with nano-$CaCO_3$ and EPDM firstly melt mixing have much higher toughness compared with that prepared by one-step compounding route. In this study, the nano-$CaCO_3$/EPDM/PP composites filled with high content of nano-inorganic particles (> 25 wt %) were prepared by two-step compounding route, and the micro morphology development of this ternary system during melt mixing was studied. It was found that the nano-$CaCO_3$ migrated from the elastomer dispersed phase to PP matrix firstly, and then accumulated to the region nearby the interface of EPDM and PP. Based on it, the toughening mechanism of the ternary composite prepared by two-step compounding route was discussed.

EXPERIMENTAL

Materials

Polypropylene (PP, T30S, MFR: 3.5 g/10 min, homopolypropylene) was manufactured by Sinopec Zhenhai Refining and Chemical, China. The precipitated calcium carbonate coated with fatty acids was purchased from Solvay, with the diameter of 40–70 nm (Winnofil's PM). Nordel IP EPDM3745P rubber was supplied by DuPont Dow Elastomers, with Mooney viscosity 45 (ML 1 + 4 at 125°C, ASTM D-1646).

Preparation of composites

At first, master batch composed of nano-$CaCO_3$ and EPDM was mixed in Brabender type plastic hot mixing machine manufactured by Eastern Engineering, Southern Korea, rotation speed of rotor was 60 rpm, and mixing temperature was 140°C. The composite composed of the master batch and polypropylene was mixed in the same mixing machine at 170°C. Rotation speed of rotator was 60 rpm and mixing time was 15 min.

The composite was molded into plate (100 × 120 × 4 mm^3) in hot press machine (QLB-25Q/D, Wuxi No.1 Rubber and Plastic Machinery, China) at 185°C for 15 min, pressure was 10 MPa, and then the plate was cut into strips for toughness test (63.5 × 12.7 × 4 mm^3). The Izod impact bars were notched with a notch cutter to a notch depth of 2.54 mm, in accordance with ASTM D-256.

Measurement

The morphologies of the ternary composites were characterized by transmission electron microscopy (TEM). Thin sections were microtomed and stained with ruthenium tetroxide (RuO_4) to enhance contrast between the PP phase and EPDM phase. All observations were carried out on a JEOL JEM-1230 TEM running at an accelerating voltage of 100 kV.

The contact angle was measured by the contact angle measurement system OCA 20, according to the sessile drop method. PP and EPDM samples for contact angle measurement were compression molded between clean silicon wafers at 200°C for 3 min and then cooled to 25°C under pressure for 1 min. Nano-$CaCO_3$ powders were compression molded by using a special mold at room temperature under pressure of 10 MPa. Contact angles were measured on 5 μL of wetting solvent at 20°C.

An XJ-300A impact tester (Gansu, China) was used for measuring the notched Izod impact strength, in accordance with ASTM D-256.

Scanning electronic microscope (SEM, S-4700, HITACHI, Japan) was used to investigate the morphology of fracture surface of the impact specimen, the fresh surface to be investigated was coated with gold, and the accelerating voltage was 15 kv.

RESULTS AND DISCUSSION

Morphology and selective particle distribution

The TEM images of nano-$CaCO_3$/EPDM/PP composites with different mixing time during the second compounding are shown in Figure 1. In the images, the light color region represented PP matrix, and the gray domains and the dark particles were EPDM dispersed phase and nano-$CaCO_3$ particles, respectively. After being mixed for 5 min, lots of large nano-$CaCO_3$ aggregates are found in PP matrix while only a few are dispersed in the vicinity of the EPDM phase, as shown in Figure 1(a). With the increase of mixing time, nano-$CaCO_3$ particles migrate from PP matrix to the vicinity of the EPDM phase [see Fig. 1(b)]. After 25 min during the second compounding, it is surprising that a large number of nano-$CaCO_3$ particles concentrated around EPDM dispersed phase, as shown in Figure 1(c).

The morphologies of multiphase polymer blends are determined by many factors, including melt viscosity of polymer components, interfacial tensions, the magnitude of shear stress and so on.[14] For polymer blends, shear stress and rheological behavior of

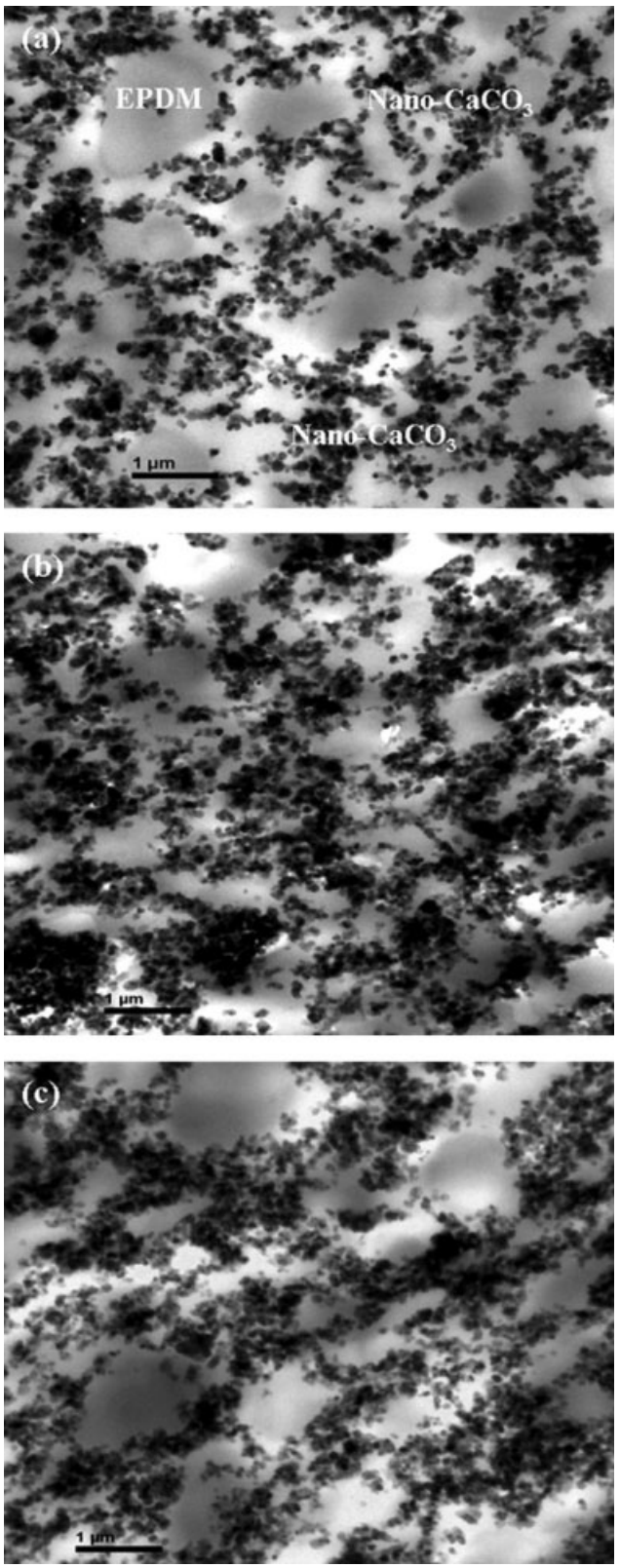

Figure 1 Phase structures of nano-$CaCO_3$/EPDM/PP (37/13/50) composites at different mixing time during the second compounding: (a) 5 min; (b) 15 min; (c) 25 min.

each polymer phase play an important role in the final phase structure.[14] The development of phase structure of nano-$CaCO_3$/EPDM/PP can be expressed by the migration of the nano-$CaCO_3$ particles. For nano-$CaCO_3$/EPDM/PP composites prepared by two step compounding route, nano-$CaCO_3$ particles are first dispersed in EPDM phase. During the second compounding, the EPDM/ nano-$CaCO_3$ compounds are teared up by the shear stress, and then nano-$CaCO_3$ particles migrate from the higher melt viscosity phase (EPDM) to the lower melt viscosity phase (PP), which is believed to be caused by the minimization of the dissipative energy.[16] As a result, nano-$CaCO_3$ particles have migrated from EPDM phase to PP phase during 5 min of mixing. With the increase of mixing time, nano-$CaCO_3$ particles begin to migrate to the interface between EPDM dispersed phase and PP matrix. The phenomenon of selective particle distribution was also discovered in the study by Dai et al.[17] This anomalous phenomenon can be explained by the interfacial tension[18] and the Young's equation. The interfacial tension can be calculated from the surface tension of the components using the harmonic mean equation of Wu[19]

$$\gamma_{12} = \gamma_1 + \gamma_2 - 4\left[\frac{\gamma_1^d\gamma_2^d}{\gamma_1^d + \gamma_2^d} + \frac{\gamma_1^p\gamma_2^p}{\gamma_1^p + \gamma_2^p}\right] \quad (1)$$

where γ^d and γ^p are the dispersive and polar term, respectively. The contact angles with water and diiodomethane are listed in Table I. Then, the surface tension, dispersion and polar components of the materials can be estimated from the contact angle data by using eq. (1).

And then the interfacial tension of each pairs can be calculated from surface tension by using the geometric mean eq. (2)[19]

$$\gamma_{12} = \gamma_1 + \gamma_2 - 2\left(\gamma_1^d\gamma_2^d\right)^{1/2} - 2\left(\gamma_1^p\gamma_2^p\right)^{1/2} \quad (2)$$

Where γ_{12} is the interfacial tension, γ_1 and γ_2 are the surface tensions of the two materials in contact. The calculated interfacial tensions of all possible pairs are given in Table II.

It is widely accepted to use Young's equation to predict particle selective distribution in a polymer blend, which was suggested by Sumita et al.[20] for the first time:

$$w_\alpha = \frac{\gamma_{\text{particle}-\beta} - \gamma_{\text{particle}-\alpha}}{\gamma_{\alpha\text{-}\beta}} \quad (3)$$

Where w_α is the wetting coefficient, $\gamma_{\text{particle-}\alpha}$, $\gamma_{\text{particle-}\beta}$, and $\gamma_{\alpha\text{-}\beta}$ are, respectively, the interfacial tension between particle and α-polymer, between particle and β-polymer, and between α- and β-polymers.

TABLE I
Contact Angle and Surface Tension Results of PP, EPDM, and Nano-$CaCO_3$ particles

Sample	Contact angle (°)		Surface tension (mN/m)		
	Water	diiodomethane	Total (γ)	Dispersion component (γ^d)	Polar component (γ^p)
PP	103.8	57.9	30.12	30.03	0.09
EPDM/3745	98.7	49.9	34.53	34.28	0.25
Nano-$CaCO_3$	95.3	22.8	47.92	47.91	0.01

Particles are expected to be selectively located in one of two polymer phases where the polymer has a higher interaction with the particle surface: $w_\alpha > 0$, that is $\gamma_{\text{particle-}\beta} > \gamma_{\text{particle-}\alpha}$, particles in α-polymer or at the interface; $w_\alpha < 0$, that is $\gamma_{\text{particle-}\beta} < \gamma_{\text{particle-}\alpha}$, particles in β-polymer or at the interfaces. In our ternary system of nano-$CaCO_3$/EPDM/PP composites, calculated wetting coefficient is listed in Table III.

From this calculation, in PP/EPDM matrix, nano-$CaCO_3$ is predicted in the EPDM phase. Namely, in this system, after a short time of mixing, nano-$CaCO_3$ particles migrated from EPDM phase to PP phase are most likely to be encapsulated by EPDM with the increase of mixing time. However, because of the higher melt viscosity phase of EPDM, nano-$CaCO_3$ particles cannot migrate into the EPDM dispersed phase. As a result, the nano-$CaCO_3$ particles accumulate selectively around the EPDM dispersed phase. In addition, because of the high content of nano-$CaCO_3$, a part of the nano-$CaCO_3$ particles are also dispersed in the PP matrix, as shown in Figure 1(c).

With the nano-$CaCO_3$ particles accumulating around the EPDM dispersed phase, the degree of aggregation for nano-$CaCO_3$ particles increases. The big nano-$CaCO_3$ agglomerates at the interface between PP and EPDM will initiate crack when the composites is subjected to stresses or energies large enough to exceed the crack growth resistance of the big nano-$CaCO_3$ agglomerates. Figure 2 shows the relationship between the Izod impact strength and the mixing time during the second compounding for the ternary composite. It can be found that the impact strength of the composite is decreased gradually with increase of mixing time. The result is in accordance with the discussion of the morphology development for the ternary composite.

TABLE II
The Value of Interfacial Tension of Nano-$CaCO_3$/EPDM/PP Composites

System	Possible pairs	Interfacial tension (γ_{12}) (mN/m)
PP/EPDM/$CaCO_3$	PP/EPDM	0.18
	PP/nano-$CaCO_3$	2.12
	EPDM/nano-$CaCO_3$	1.30

Izod impact strength and toughening mechanism

The influence of the nano-$CaCO_3$ content on the impact strength of the ternary composite by two step compounding route is shown in Figure 3. With the increase of the nano-$CaCO_3$ loading, the Izod impact strength of the ternary composite is remarkably enhanced. In the case of the same PP : EPDM ratio, a ternary composite with Izod impact strength about two times higher than PP/EPDM binary blends has been achieved by adding 15–30 wt % nano-$CaCO_3$ particles. In the case of the same nano-$CaCO_3$: EPDM ratio, a ternary composite with Izod impact strength about 12–16 times higher than pure PP has also been achieved by adding 25–40 wt % nano-$CaCO_3$ particles. The results show that there must exist a synergistic toughening effect between nano-$CaCO_3$ particles and EPDM on nano-$CaCO_3$/EPDM/PP composites.

The SEM images of the fracture surface of nano-$CaCO_3$/EPDM/PP composites are shown in Figure 4. In Figure 4, the nano-$CaCO_3$ agglomerates are clearly visible. The size of the nano-$CaCO_3$ agglomerates is in the range of 0.5–3 μm. From these images, it can be clearly observed that there are more nano-$CaCO_3$ agglomerates in Figure 4(b,b′) compared with that in Figure 4(a,a′). In addition, with the increase of nano-$CaCO_3$ in the composites, the size of nano-$CaCO_3$ agglomerates increases.

In Figure 4, it can be also found that a lot of fibrils exist at the interphase between nano-$CaCO_3$ agglomerates and matrix obviously [see Fig. 4(a′,b′)]. When the composites is subjected to external stress, the

TABLE III
Wetting Coefficient (w_α) in Ternary System of Nano-$CaCO_3$/EPDM/PP Composites

α phase	β phase	w_α
PP	EPDM	4.55

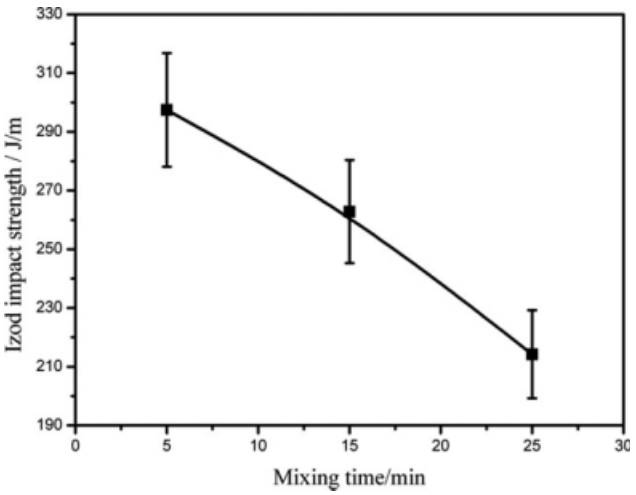

Figure 2 Izod impact strength of nano-$CaCO_3$/EPDM/PP composites (37/13/50) as a function of mixing time during the second compounding.

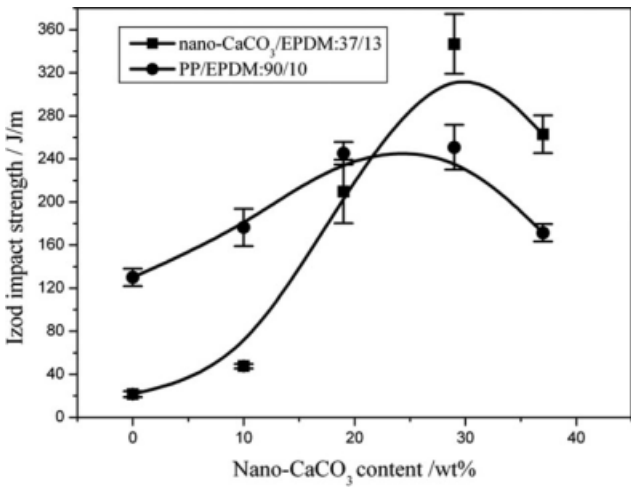

Figure 3 Izod impact strength of nano-$CaCO_3$/EPDM/PP composites as a function of the nano-$CaCO_3$ content.

bigger nano-$CaCO_3$ agglomerates act as stress concentration, resulting from the different elastic properties and the distinguishing Poisson's ratio from the matrix. At the same time, separation process occurs at the interphase between the matrix and nano-$CaCO_3$ agglomerates. Because of the surface treatment with fatty acids, nano-$CaCO_3$ agglomerates

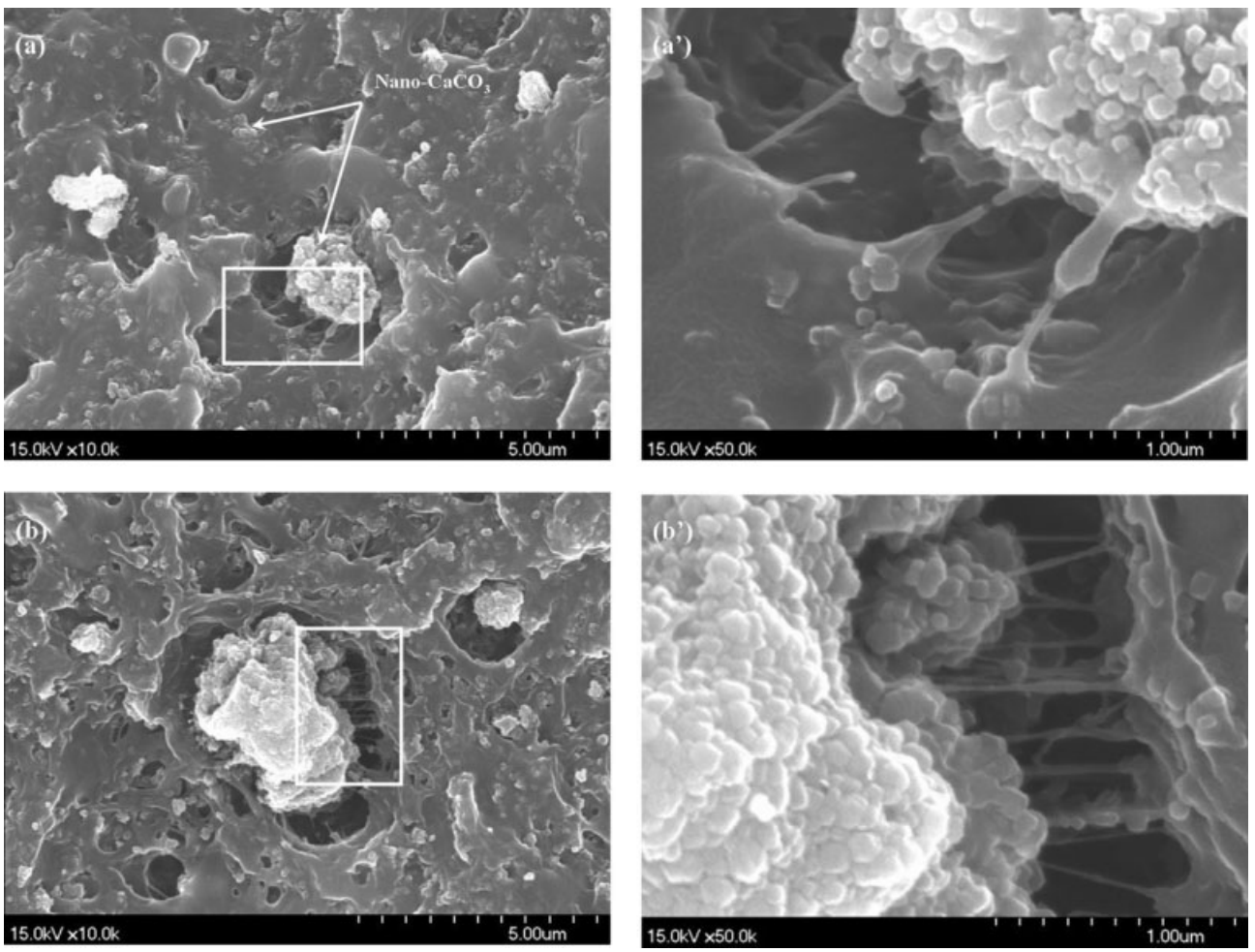

Figure 4 SEM images of the impact fracture of nano-$CaCO_3$/EPDM/PP ternary composites: (a, a′) two–step compounding route, nano-$CaCO_3$/EPDM/PP = 29/10/61; (b, b′) two–step compounding route, nano-$CaCO_3$/EPDM/PP=37/13/50.

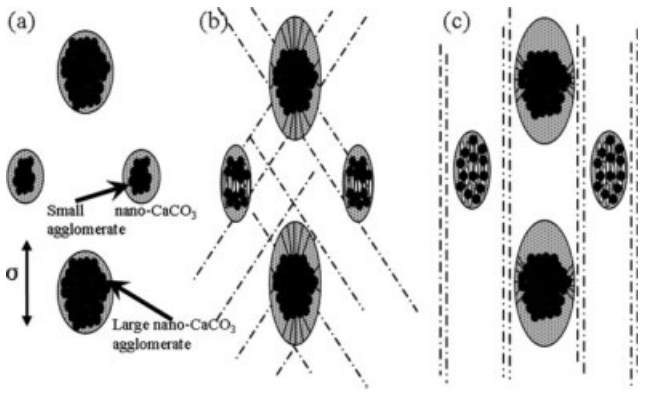

Figure 5 Schematic drawing of the micromechanical deformation process: (a) stress concentration, (b) void and shear band formation, (c) induced shear yielding.

have good compatibility with the PP matrix. Therefore, when the separation process occurs, matrix is stretched to form fibrils. This fibrillation process can dissipates lots of energy.

Mechanical properties of the composites are determined not only by the components, but also by the phase structure. Kim et al.[8,21,22] explored the toughen mechanism of particle filled semi-crystalline polymers by studying the micromechanical deformation process. A three-stage mechanism is put forward in the study by Kim et al. In the first stage, stress concentration takes place around the modifier particles, resulting from its different elastic properties from the matrix. In the second stage, micro voids form through cavitation inside particles or debonding at the particle matrix interface with further increasing strain. Simultaneously, weak shear bands form in the matrix between the particles. In the third stage, shear flow in the matrix will be accelerated as increase of the void size.

In our nano-$CaCO_3$/EPDM/PP composites with high content of nano-$CaCO_3$, dispersed EPDM phase and nano-$CaCO_3$ agglomerates coexist in the PP matrix. According to the TEM images of Figure 1, it can be clearly observed that neither of the dispersed components exhibits any tendency to spread on the other. When EPDM dispersed phase is surrounded by PP, this kind of micromechanical deformation process is defined as a fibrillized debonding process at the interface.[8] Although the nano-$CaCO_3$ agglomerate is surrounded by PP, the kind of micromechanical deformation process can be divided into two situations, namely the large nano-$CaCO_3$ agglomerate and the small nano-$CaCO_3$ agglomerate. Figure 5 is the schematic drawing of the micromechanical deformation process. During the deformation process, the stress concentration occurs first around the large nano-$CaCO_3$ agglomerate [see Fig. 5(a)]. Because of the smaller specific surface areas at the interface, with further increase in strain, separation process at the interface between nano-$CaCO_3$ agglomerate and PP matrix occurs at first on the polar region propagating to the equatorial region of nano-$CaCO_3$ agglomerate [see Fig. 5(b)]. Because of a certain phase adhesion, a few fibrils exist at the interface [see Fig. 4(a′,b′)]. In connection with these debonding processes, the PP matrix between the voids deforms more easily to obtain a shear band [see Fig. 5(c)]. When the small nano-$CaCO_3$ agglomerate is surrounded by PP matrix, because of the small interparticle distance between nano-$CaCO_3$ particles, shear flow process, and fibrillation can be easily activated in the thin PP matrix bands between the particles [see Fig. 5(b)]. As a result, if the PP matrix distance between the aggregates is sufficiently small, the PP matrix can be further deformed through the shear flow [see Fig. 5(c)].

CONCLUSION

Nano-$CaCO_3$/EPDM/PP composites with the high content of nano-$CaCO_3$ were prepared by two-step compounding route. The impact strength, phase morphology, and interfacial tension of the ternary composite were investigated. The TEM images show that nano-$CaCO_3$ particles transported from EPDM to PP matrix firstly and then from PP to the vicinity of EPDM dispersed phase with the increase of mixing time during the second compounding. The micromorphology observation also shows that lots of nano fibrils existed at the interface between nano-$CaCO_3$ agglomerate and PP matrix, which can dissipate lots of energy and may also initiate shear band in the matrix. The relationship between Izod impact strength and nano-$CaCO_3$ concentration indicates that increasing the nano-$CaCO_3$ concentration can increase the toughness of the ternary composite obviously. The impact strength of nano-$CaCO_3$/EPDM/PP composites reaches the maximum value when the nano-$CaCO_3$ content reached 29 wt %. Satisfied toughening effect can still be obtained in this ternary composite with the loading of 37 wt % nano-$CaCO_3$.

References

1. Zhao, M.; Gao, J. G.; Deng, K. L.; Zhao, X. Y. Modified Polypropylene Material, Chemical Industry Press: Beijing, 2002.
2. Ma, C. G.; Zhang, M. Q.; Rong, M. Z. J Appl Polym Sci 2007, 103, 1578.
3. Ma, C. G.; Mai, Y. L.; Rong, M. Z.; Ruan, W. H.; Zhang, M. Q. Compos Sci Technol 2007, 67, 2997.
4. Wang, X.; Sun, J.; Huang, R. J Appl Polym Sci 2006, 99, 2268.
5. Zhang, L.; Li, C. Z.; Huang, R. J Polym Sci Pol Phys 2005, 43, 1113.
6. Premphet, K.; Horanont, P. J Appl Polym Sci 2000, 76, 1929.
7. Premphet, K.; Horanont, P. Polymer 2000, 41, 9283.
8. Kim, G. M.; Michler, G. H. Polymer 1998, 39, 5699.
9. Shanks, R. A.; Long, Y. Polym Network Blend 1997, 7, 87.

10. Yang, H.; Zhang, X.; Qu, C.; Li, B.; Zhang, L.; Zhang, Q.; Fu, Q. Polymer 2007, 48, 860.
11. Marosi, G.; Lagner, R.; Bertalan, G.; Anna, P.; Tohl, A. J Therm Anal 1996, 47, 1163.
12. Varga, J. J Polym Eng 1991, 10, 231.
13. Szlezyngier, W. Przem Chem 1991, 70, 32.
14. Pukanszky, B.; Tudos, F.; Kolarik, J.; Lednicky, F. Polym Compos 1990, 11, 98.
15. Hanim, H.; Fuad, M. Y. A.; Zarina, R. Z.; Ishak, A. M.; Hassan, A. J Thermoplast Compos 2008, 21, 123.
16. Persson, A. L.; Bertilsson, H. Polymer 1998, 39, 5633.
17. Dai, K.; Xu, X. B.; Li, Z. M. Polymer 2007, 48, 849.
18. Vankrvelen, D. W. Properties of Polymers; Elsevier: Amsterdam, 1976; Chapters 4 and 5.
19. Wu, S. Polymer Interface and Adhesion; Marcel Dekker, Inc: New York, 1982.
20. Sumita, M.; Sakata, K.; Asai, S.; Miyasaka, K.; Nakagawa, H. Polym Bull 1991, 25, 265.
21. Kim, G. M.; Lee, D. H. J Appl Polym Sci 2001, 82, 785.
22. Kim, G. M.; Michler, G. H. Polymer 1998, 39, 5689.